JOURNAL OF MATERIALS SCIENCE **40** (2005) 4355–4364

Single fibre pullout tests on auxetic polymeric fibres

V. R. SIMKINS, A. ALDERSON, P. J. DAVIES, K. L. ALDERSON*
CMRI, The University of Bolton, Bolton, Lancashire, UK
E-mail: ka1@bolton.ac.uk

A novel route for production of auxetic fibres has been adapted from conventional melt extrusion techniques. These fibres were reproduced, characterised and tested, for the first time, to assess the potential of auxetic fibres as reinforcements in composite materials. Initial experimental work has included the embedding of single fibres in modified epoxy resin. Auxetic fibre specimens were then compared with conventional fibre specimens through a specially designed fibre pullout testing procedure. The auxetic specimens displayed superior anchoring properties. The average maximum force at de-bonding of the auxetic fibres (0.95 N) was observed to be over 100% higher than that for conventional ones (0.44 N) and the average energy required to fully extract the auxetic fibre from the modified resin was 8.3 mJ while the conventional fibre required only 2.5 mJ on average. The results indicate that composites employing auxetic fibres as the reinforcement phase will exhibit enhanced resistance to failure due to fibre pullout.

1. Introduction

Auxetic materials are those which possess a negative Poisson's ratio (ν)—that is, they undergo transverse expansion when under axial tensile load, unlike most materials which contract under the same loading conditions, e.g. a rubber band or chewing gum. Poisson's ratio is defined:

$$\nu_{xy} = -\varepsilon_y/\varepsilon_x \tag{1}$$

where ε_x is tensile strain in the loading direction while ε_y is the tensile strain perpendicular to this. Although naturally auxetic materials do exist [1–3] most materials have $\nu \cong +0.25$ to $+0.33$. Exceptions to this include cork which has a Poisson's ratio of 0 and rubber which has a Poisson's ratio of $\approx +0.5$. Auxetic materials are predicted to offer potential enhancements in a range of important properties. For example, the indentation resistance H of isotropic materials is predicted to be enhanced [4, 5] due to the relationship

$$H \propto (1 - \nu^2)^{-x} \tag{2}$$

where the value of x varies according to the analytical theory used, and

$$-1 \leq \nu \leq +\frac{1}{2} \tag{3}$$

for isotropic materials. Looking at the two extremes, if an isotropic material with $\nu = -1$ could be obtained as opposed to one with $\nu = +0.5$, then it can be seen from Equation 2 that the hardness would be predicted to be substantially enhanced. This has now been examined in foams, microporous polymers and composites and enhancements of up to 4 times over conventional materials have been seen [6].

Lakes' work, in 1987, with polymeric re-entrant foams [4] was the first documented synthesis of an auxetic material and subsequently has inspired further work into the synthesis of auxetic polymeric materials. This was given impetus by the discovery of a nodule-fibril microstructure in an already available microporous, anisotropic form of expanded polytetrafluroethylene (PTFE) with auxetic properties [7]. Its Poisson's ratio value varied with strain and negative values as large as -12 were measured. Following Caddock and Evans' findings in microporous PTFE there was interest in the possibility of synthetically producing nodule-fibril microstructures in other polymeric materials.

A patent application was made by Evans and Ainsworth [8] to cover the production route for polymers having a microstructure comprising of nodules and fibrils, leading to a negative Poisson's ratio. They fabricated auxetic polymers in the form of cylinders or rods. The production route of these rods incorporated compaction [9], sintering [10] and extrusion [11] stages with careful temperature management. During this work, an examination of the morphology of the powder used as a starting point for manufacture was carried out and it was found to be an essential component in the successful synthesis of auxetic ultra high molecular

*Author to whom all correspondence should be addressed.

weight polyethylene (UHMWPE) and polypropylene (PP) [12]. For auxetic PP, for example, a finely divided powder with average particle-size distribution between 50 and 300 μm, with irregular shape and rough surfaces was found to produce the best results.

As a development of the latter work, polypropylene filaments were melt-extruded to exacting conditions which allowed the production of filaments with auxetic character [13, 14]. The importance of the fibre work lay in the need to produce auxetic polyolefins in a form that lent itself more readily to applications-based research. The principles used in the ram-extrusion production route for the rods were the basis of the work. However, continuous production of fibres, using an extruder of Archimedian screw principle, cannot allow for a separate compaction stage. The static sintering stage used in the rod work [10, 12] was adapted to this extrusion method by reducing the throughput speed. This allowed the material to move slowly through the extruder's 3 barrel zones before reaching the adapter or die zones, where it emerged with no drawing apart from that caused by gravity as the fibres exited the spinneret [14].

Characterisation of these fibres included Scanning Electron Microscopy (SEM), Differential Scanning Calorimetry (DSC), Video Extensometry (VE) and tensile testing. The auxetic fibres were found to be auxetic with a typical Poisson's ratio value of $\nu = -0.6$ [14]. Conventional fibres were also produced, with a typical Poisson's ratio of $\nu = +0.34$.

The primary objective of this work is, by experiment, analysis and modelling, to investigate the predicted benefits of using auxetic fibres as fibre reinforcements in composite materials [5, 15]. Premature failure of composite materials due to crack propagation and fibre pullout is seen as a limiting factor. The nature of an auxetic material to expand when being stretched is predicted [5, 15] to assist in the control and delay of fibre pullout as shown in Fig. 1.

In relation to fibre pullout behaviour, the majority of researchers reviewed [16–24] have been concerned with the highly complex behaviour of the fibre-matrix interface, the propagation of interfacial failure and the stresses and elastic behaviour of the immediate matrix area during the fibre pull-out event. The successful development of auxetic fibres [14] now enables a new approach to minimising failure due to fibre pullout. Hence, this work focuses upon a comparison of the fibre pullout performance of auxetic fibres and the conventional fibres.

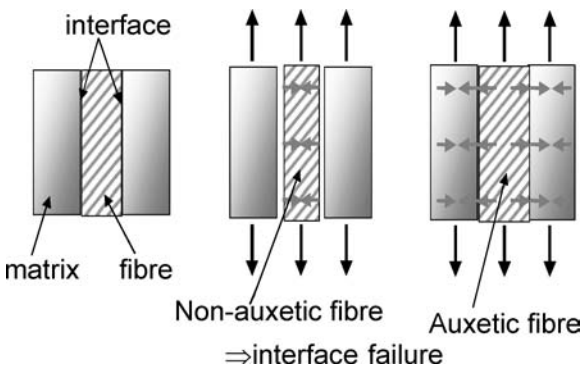

Figure 1 Predicted anchoring effect provided by auxetic fibre when under tensile load. The negative Poisson's ratio causes the fibre to expand instead of contract - maintaining interfacial contact for longer.

To assess the quality of the fibre-matrix interface, there are many variations on four basic characterisation methods or micro-mechanical tests, which are single fibre pullout, micro-bond, fibre push-out and indentation or push-down.

In the single fibre pullout test the fibre end is partially embedded in a resin matrix and the matrix is then held stationary on a solid base while the fibre is pulled out. This was selected as the most suitable method for this work, since the mechanisms of fibre pullout of auxetic fibres are what the work set out to assess.

A method of fibre pullout was developed, based on the work of Betz [16], and the pullout performance of auxetic and conventional fibres was assessed. It was found that the auxetic fibres required up to twice as much external force to reach the peak of de-bonding and that the energy required to complete pullout of auxetic fibres was, on average, three to four times that required for the conventional fibres.

2. Experimental methods

2.1. Production of auxetic fibres

In accordance with the patented manufacturing process [13] polypropylene fibres were produced using the same powder used by Pickles *et al.* [12] to produce PP rods. This was grade PB0580 produced by Plast-Labor S.A. and supplied by Univar plc. The melt extrusion process was performed using an Emerson and Renwick Ltd Labline extruder, (Fig. 2), which has five thermostatically controlled temperature zones, a 3:1 compression ratio and a 25.4 mm diameter screw of length/diameter ratio 24:1. Screw speed was set to 1.05 rad s^{-1} with a take-off speed of 0.032 m s^{-1}, using cooled rollers. A batch of conventional fibres was produced as a comparative control with temperature zones set to 180, 185, 190, 195 and 200°C respectively. The auxetic fibres were produced under exactly the same conditions except that the temperature profile was amended to 159°C across all zones.

2.2. Characterisation of fibres

In order to fully characterise the fibres, a number of tests were carried out. Fibre diameter was measured using both an engineer's micrometer and a graticule of 0.01 mm scale. Ten measurements were taken evenly spaced along each of ten 120 mm fibre specimens. This was done for both auxetic and conventional specimen types. The two types of measurement were found to be within ~20 microns (10%) error. An average value was obtained from these measurements. Then, the density was determined by measuring 3 samples of 10 metres of fibre, weighing each individual length on electronic weighing scales accurate to 0.001 g and referring to the diameter measurements taken earlier. The mechanical properties were determined through tensile testing using Instron 4303 equipment, fitted with 100 N load

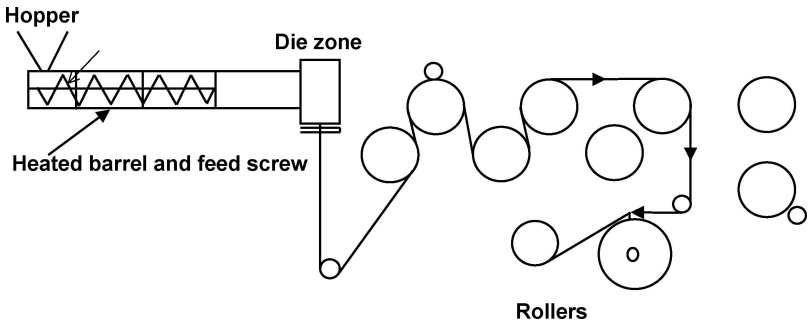

Figure 2 Schematic of extruder set up used to produce fibres for this work.

cell, situated in an environmentally controlled room at 65%relative humidity and a temperature of 23°C. Gauge-length and grip-distance were set to 50 mm with travelling speed of 25 mm min^{-1}. Finally, the Poisson's ratio was determined using Biax 200C micro-tensile testing equipment, which was fitted with 10 Newton load-cell and a Messphysik video extensometry package as described in the earlier paper [14].

2.3. The design and preparation of a resin matrix

Due to the auxetic fibres' thermal characteristics [25], the matrix material was selected carefully to avoid introducing an extra variable. Since the fibres possessing a negative Poisson's ratio were produced at 159°C, the matrix had to be a cold-cure resin and was also needed to produce only a low exotherm during setting, of 140°C or less.

It was necessary to modify the resin to a point where the fibre may be removed from the matrix or the fibre-matrix interface failed before the fibre itself reached its elastic limit and began necking. The single fibre pull-out comparisons made between the auxetic and conventional fibres required the careful design of a model composite which took into account the tensile characteristics of the fibres themselves.

The material selected for the matrix was a cold-cure epoxy resin, Araldite LY 5052 with hardener HY 5084. Properties of the unmodified, cured, neat resin casting (non-reinforced) when gelling and curing at room temperature are given in Table I. Dibutyl phthalate was used to inhibit the resin's ability to form cross-links in the curing process, by a process developed in house.

TABLE I Properties of non-modified epoxy resin used for matrix

Araldite LY5052/HY5084 cold cure epoxy	
Tensile strength	60–63 MPa
Strain at tensile strength	2.3–3.0%
Tensile stress at rupture	58–62 MPa
Strain at rupture	2.4–3.2%
Tensile modulus	3.1–3.2 GPa
TG_{onset}	52°C
TG	56°C
Flexural strength	80–85 MPa
Strain at flexural strength	2.8–3.1%
Flexural stress at rupture	80–85 MPa
Strain at rupture	2.9–3.1%
Tensile modulus	2.95–3.05 GPa

The amount of dibutyl phthalate added to the resin mixture started at 2.75×10^{-6} m^3 and increased by 2.75×10^{-6} m^3 increments for each resin mixture up to 41.25×10^{-6} m^3. Table II shows the resin mixtures considered.

44.25 g of resin was weighed carefully in a plastic beaker using electronic scales accurate to 1×10^{-5} g, the relevant quantity of plasticiser was added and thoroughly mixed with the resin. The hardener was added last, as 10.2 g, and thoroughly blended with the resin/plasticiser mixture. Resin coupons measuring 12.7 mm × 60 mm × 3 mm, and a model single fibre pullout specimen of each resin mixture were made and cured at room temperature. These pairs were then individually subjected to tensile loading and results were collated and analysed until the desired fibre matrix pull out behaviour was observed.

2.4. Single fibre pullout specimen preparation

A clear polystyrene bijou tube with flat internal base, Fig. 3A, was pierced centrally in the base with a 0.5 mm drill. An auxetic fibre was threaded carefully through the hole and secured with BluTak® in the external recess of the base, Fig. 3B. The tube and fibre were then carefully inserted into one of the holes in a specially built loading rack, Fig. 3C. The fibre was then held vertical by inserting it into a hole, machined central to the axis of the tube and fibre. The fibre was held in place with BluTak® on the top surface of the hole.

Taking great care to avoid contamination of the free fibre end, a syringe containing a 3×10^{-6} m^3 measured quantity of prepared resin mixture was used to charge the tube, via an access hole formed in the top of the loading rack, Fig. 3D. The loading rack was then kept in a warm room with ambient temperature of 24°C ± 2°C. A gel time of 6 h at room temperature was allowed followed by seven days curing time in the same conditions [26]. The 3×10^{-6} m^3 of resin gave an embedded fibre length of 20 mm.

When the model composite had completed its curing time, it was carefully removed from the loading rack, the BluTak® was removed and a new razor blade was used to shear the protruding fibre from the base, level with the surface of the plastic tube. The free fibre end was carefully held, to avoid compressive damage or tensile loading. Pullout specimens made using the different resin types, Table II, were tested (using experimental parameters described in 'Fibre pullout tests').

TABLE II Resin matrix midifications attempted. Bold figures indicate most successful recipe used for all following work

LY5052 ($\times 10^{-6}$ m^3)	LY5052 (g)	HY5084 ($\times 10^{-6}$ m^3)	HY5084 (g)	Dibutyl Phthalate ($\times 10^{-6}$ m^3)	Dibutyl Phthalate (g)	Total Volume ($\times 10^{-6}$ m^3)	Total Weight (g)	Dibutyl Phthalate Volume(%)	Dibutyl Phthalate Weight(%)
40	44.24	9.20	10.176	2.75	2.89	51.95	57.31	5.29	5.04
40	44.24	9.20	10.176	5.50	5.78	54.70	60.20	10.06	9.60
40	44.24	9.20	10.176	8.25	8.67	57.45	63.09	14.36	13.74
40	44.24	9.20	10.176	11.00	11.56	60.20	65.98	18.27	17.52
40	44.24	9.20	10.176	13.75	14.45	62.95	68.87	21.84	20.98
40	44.24	9.20	10.176	16.50	17.34	65.70	71.76	25.12	24.17
40	44.24	9.20	10.176	19.25	20.23	68.45	74.65	28.12	27.10
40	44.24	9.20	10.176	22.00	23.12	71.20	77.54	30.90	29.82
40	44.24	9.20	10.176	24.00	25.20	73.20	79.62	32.79	31.65
40	44.24	9.20	10.176	24.75	26.01	73.95	80.43	33.47	32.34
40	44.24	**9.20**	10.176	**25.00**	26.30	**74.20**	80.72	**33.69**	**32.58**
40	44.24	9.20	10.176	25.44	26.73	74.63	81.15	34.08	32.94
40	44.24	9.20	10.176	26.13	27.46	75.32	81.87	34.69	33.54
40	44.24	9.20	10.176	26.81	28.18	76.01	82.60	35.28	34.12
40	44.24	9.20	10.176	27.50	28.90	76.70	83.32	35.86	34.69
40	44.24	9.20	10.176	30.25	31.79	79.45	86.21	38.08	36.88
40	44.24	9.20	10.176	33.00	34.68	82.20	89.10	40.15	38.93
40	44.24	9.20	10.176	35.75	37.57	84.95	91.99	42.09	40.85
40	44.24	9.20	10.176	38.50	40.46	87.70	94.88	43.90	42.65
40	44.24	9.20	10.176	41.25	43.35	90.45	97.77	45.61	44.34

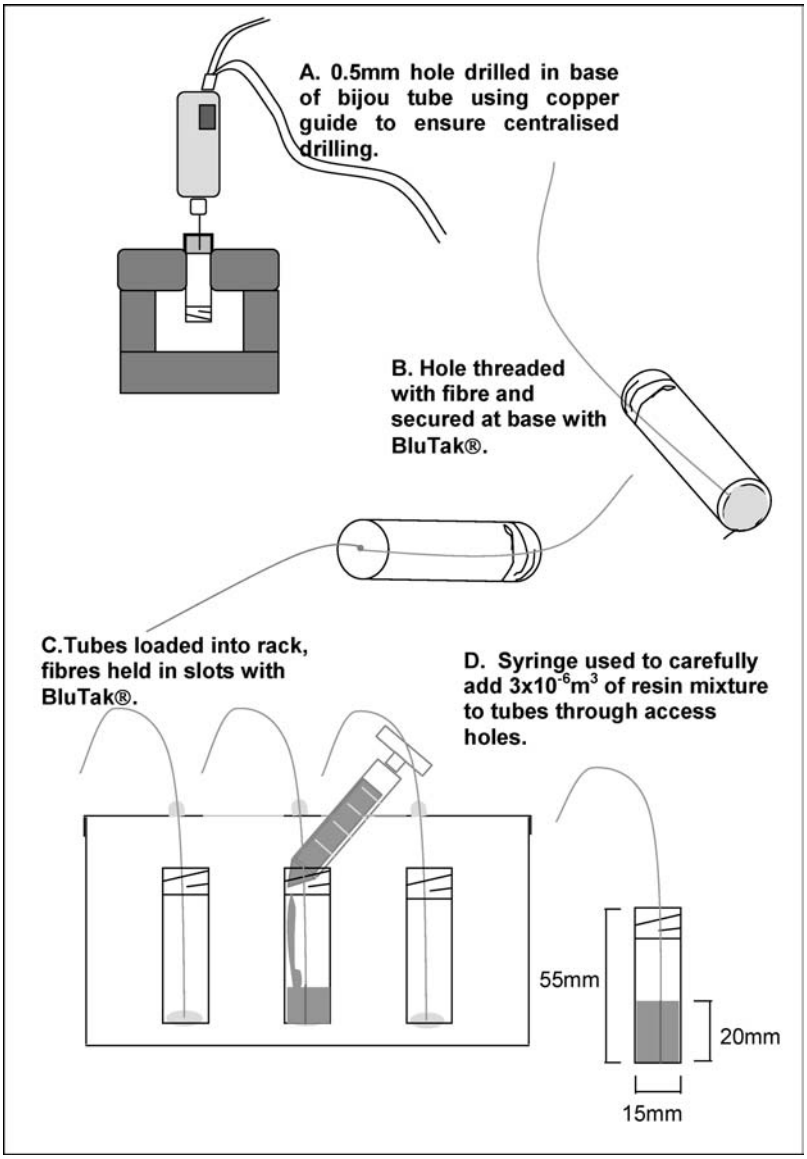

Figure 3 Schematic of single fibre pullout specimen preparation.

It was noted that the surface tension and residual stresses in the resin during setting were sufficient to pull the fibre down from the supporting frame where it was secured with BluTak®, leading to the fibre being curved at times. With this in mind, regular checks were made during the setting period to gently secure the fibres and ensure their straightness, although the problem was reduced as the inhibitor percentage increased.

Due to the possibility of air gaps, it was necessary to observe the fibre/matrix interface to judge the quality of adhesion. This was done by open-casting small lozenges of resin of the optimum formula, approximately 2 mm thickness and 10 × 50 mm, with fibres of each type laid in. These were allowed to set and cure in exactly the same manner as the pullout specimens. The samples were then cryogenically fractured (using liquid N_2) in strategic positions so fragments of the fibres would be exposed. The broken fragments were each examined microscopically. At the same time, the fragments were observed for any evidence of surface interaction between the fibre and matrix. No evidence was found of any surface interaction between the two materials in either auxetic or conventional specimens.

2.5. Fibre pullout tests

Using Instron 4200 testing equipment fitted with a 100N load cell, the specimen (still in its tube) was inverted and gripped in the collet grip, which was attached to the cross-head with a self-levelling gimble attachment, Fig. 4. The free fibre end was clamped in the lower rubber lined jaw. The grip distance was set to 70 mm, which represented the distance from the top edge of the resin in the inverted tube to the top edge of the lower grip. The gauge length was set to 20 mm, representing the fibre's embedded length. The rate of displacement was 5 mm min^{-1} and the sampling rate was 10 points per second. For each specimen, a record was made of any amount of fibre pullout (visually identifiable) and any amount of plastic deformation and necking, with measurements.

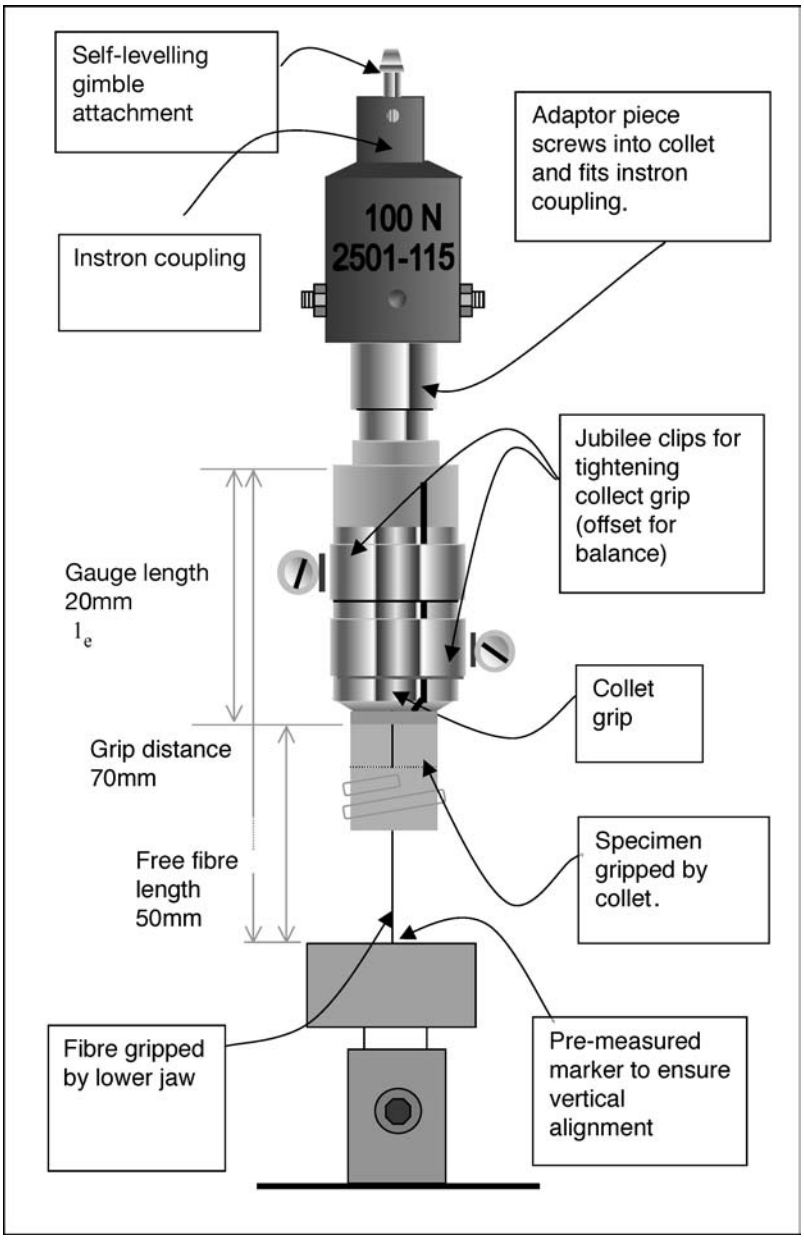

Figure 4 Schematic of single fibre pullout experimental set up.

Using these parameters the complete range of pull-out specimens was tested. When the resin containing 24.75×10^{-6} m^3 of inhibitor was tested, the fibre pulled out cleanly and without damage. Markers placed on the fibre near the resin confirmed that the fibre had pulled out without fracture or plastic deformation. Further tests were performed to confirm the best resin formula between 24×10^{-6} m^3 and 25×10^{-6} m^3 of inhibitor. These confirmed that the 25×10^{-6} m^3 quantity was the most consistent in allowing the fibre to extract as described. Consequently, this resin formula was used for all further pullout tests in this research. This formula produced a resin with a Young's modulus of 0.13 GPa and tensile strength of 0.76 MPa. Having confirmed the most suitable resin formula, two comparative sets of pullout specimens were made using auxetic and conventional fibres and tested as before.

3. Results

3.1. Fibre characterisation

The fibre characterisation methods revealed that apart from Poisson's ratio values, the two fibre types used in this work had very similar dimensions and mechanical properties (see Table III).

3.2. Fibre pullout results

Figs 5 and 6 show a selection of force-displacement curves for both auxetic and conventional fibre pull-out specimens. Typically, the auxetic fibres' peak de-bonding force remains higher over a greater displacement distance, indicating a prolonged de-bonding event. In comparison, the conventional fibres, Fig. 6, suffer much lower and sharper peak de-bonding events, requiring much less energy to pull out the fibre.

TABLE III Fibre properties compared

AUXETIC FIBRE	
Diameter	226 μm
Density (ρ)	633 kg/m^3
Young's modulus (E)	1.34 GPa
Tensile strength	28 MPa
Poisson's ratio value	-0.6 ± 0.05
CONVENTIONAL FIBRE	
Diameter	228 μm
Density (ρ)	774 kg/m^3
Young's modulus (E)	1.38 GPa
Tensile strength	32.57 MPa
Poisson's ratio value	+0.34

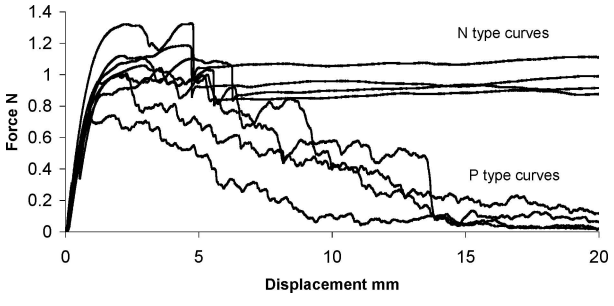

Figure 5 Auxetic fibre pullout curves.

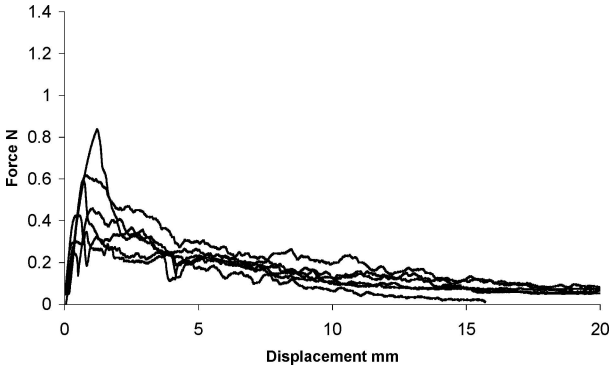

Figure 6 Conventional fibre pullout curves.

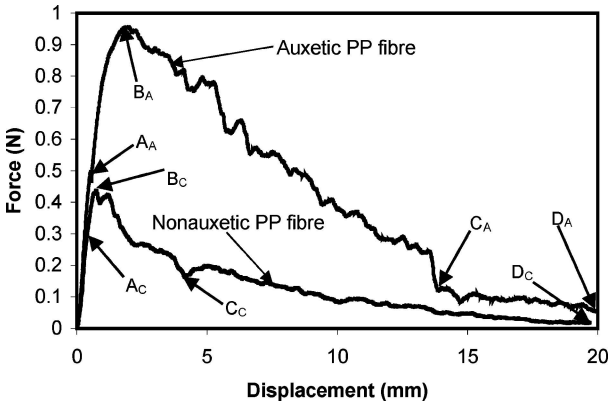

Figure 7 Average force-displacement curves compared for the conventional and auxetic single-fibre pullout tests.

The auxetic fibres exhibit two distinct types of curve as can be seen in Fig. 5; one being a typical pullout curve (referred to as Type P) and the other indicating plastic deformation (referred to as Type N). The Type N indicates an initial pullout of up to 6 mm before necking occurs at between 1.1 and 1.3 N. The Type P curves tend to decline after the peak representing complete pullout with no 'necking'.

Fig. 7 shows a direct comparison between the average auxetic Type P curves and average conventional fibre pullout curves. It can be seen that the energy used to pull out an auxetic fibre, at 8.3 mJ, is over three times greater than for pull out of the 'conventional' fibres, at 2.5 mJ.

4. Discussion

The results have shown significant improvements in fibre pullout resistance for auxetic fibres. The mechanisms responsible for this will now be discussed by considering the behaviour of the idealised conventional and auxetic single-fibre pull-out specimens at various stages of the pull-out test shown schematically in Fig. 8.

After 40 years of fibre pullout testing, analysis of the curves is still open to interpretation [27]. In the case of a weakly bonded interface, such as that found in systems containing glass fibres [28], carbon fibres [29] and Kevlar [30], a typical single fibre pull-out curve consists of 4 phases. In the initial phase a linearly increasing force-displacement curve exists, corresponding to elastic deformation of the free fibre end,

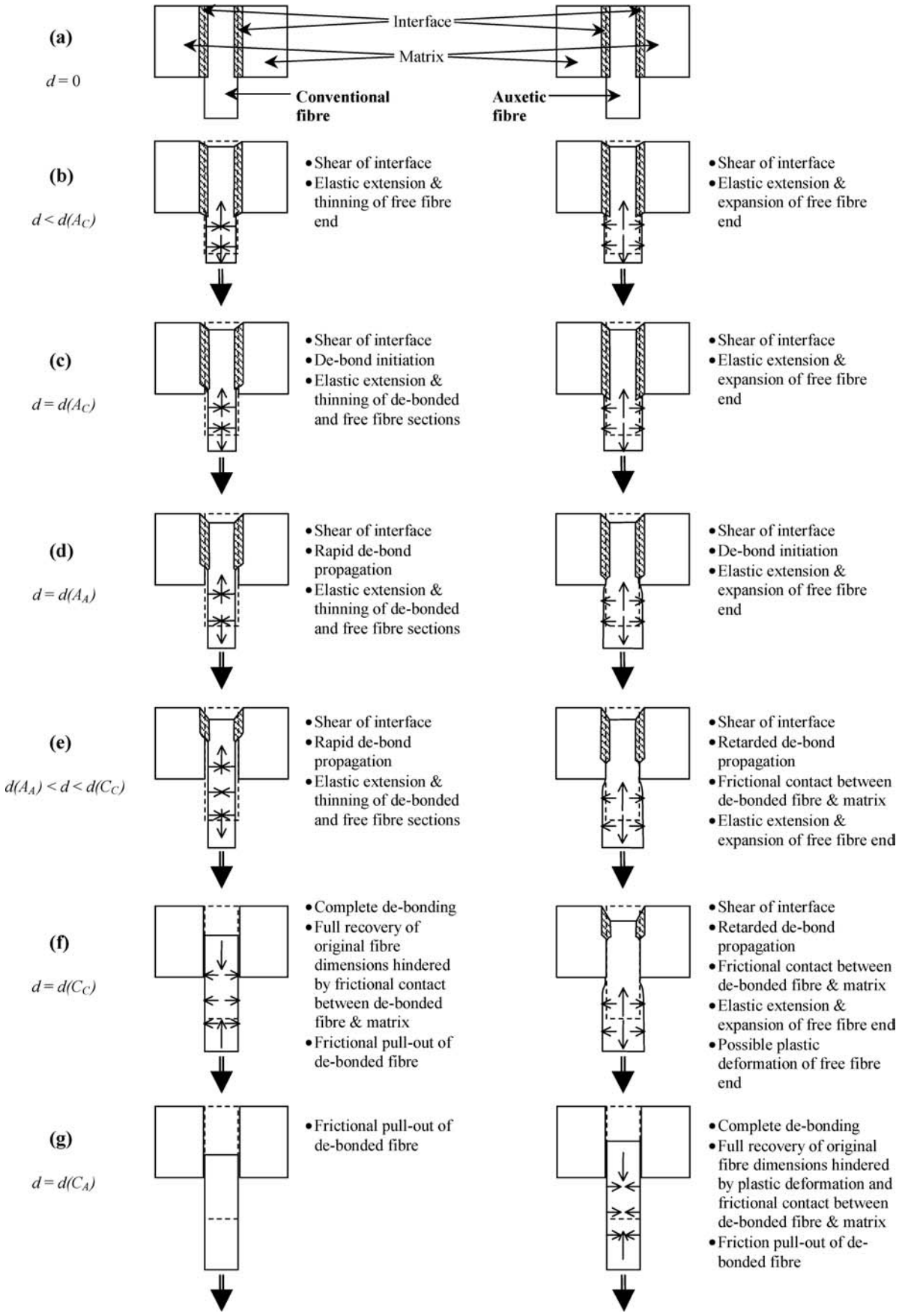

Figure 8 Schematic of the pull-out process for the conventional (left hand side) and auxetic (right hand side) single-fibre specimens. Displacements (d) correspond to points shown on Fig. 7. The original position and dimensions of the fibres are indicated by a dashed outline in each case.

elastic shear of the fibre-matrix interface, and elastic deformation of the embedded fibre end. The point (A) at which the force-displacement curve deviates from linearity defines the beginning of the second phase of the pullout behaviour, which culminates in a maximum to the force-displacement curve (B). If the work of others is followed [16–24], this represents the initial stages of interfacial failure between the fibre and matrix, in which the formation of a void or voids between the fibre and matrix occurs. The third phase of the pull-out behaviour (B-C) is characterised by a decrease in the force as the displacement increases further, and is indicative of increased fibre-matrix de-bonding at the interface, and slip-stick frictional sliding of the de-bonded region(s) of fibre as it is extracted from the resin matrix. In this region, the frictional response of the de-bonded region(s) of fibre becomes increasingly dominant (over the shear of the bonded interface) in the force-displacement curve. Frictional pullout of the completely de-bonded fibre represents the final phase (C-D) of the pull-out behaviour and is characterised by an essentially linearly decreasing force-displacement curve.

Points A-D are indicated on Fig. 7 for both the auxetic (subscript 'A') and conventional (subscript 'C') fibres.

The auxetic fibre specimen clearly displays an ability to withstand a higher peak load, which occurs at a higher displacement, and is able to sustain a higher load over the entire displacement range. In comparison, the conventional PP fibre specimen displays a much lower and sharper peak to the force-displacement curve.

The specimens used in this work were relatively soft and flexible and the free fibre length was relatively large, which is likely to be responsible for the smooth, featureless initial elastic regions (0-A) shown for both curves in Fig. 7.

For the purpose of this work the point A, at which the curve becomes non-linear, will be taken as the initiation of de-bonding [16–24, 27]. The conventional fibre specimen appears to undergo initiation of de-bonding at slightly lower load and displacement values (0.3 N and 0.4 mm, respectively) than the auxetic fibre specimen (0.5 N and 0.55 mm, respectively). This may be due to the tendency for the conventional fibre to undergo positive Poisson's ratio-induced radial contraction during the test which, therefore, acts to pull the fibre away from the matrix perpendicular to the loading direction. This will add to the effects of the applied shear stress at the interface and eventually lead to the formation of a void (initiation of de-bonding). This is shown in Fig. 8c for the case of a surface de-bond where the stress build-up will be greatest [16, 17, 21, 23, 27] for the two combined effects. The tendency for the auxetic fibre to expand radially, on the other hand, will act to maintain the integrity of the interface to higher applied loads and displacements (e.g. Fig. 8d).

The sharper peak to the force-displacement curve (0-A-B-C) for the conventional PP fibre specimen indicates a more catastrophic de-bonding of the fibre-matrix interface. This can be explained by considering the stress concentration at the tip of the de-bond at the interface, and the behaviour of the de-bonded section of fibre (Figs 8d and e). In the case of the conventional fibre, the positive Poisson's ratio-induced radial contraction acts to pull the fibre away from the matrix at the crack (de-bond) tip. This causes an increase in the stress concentration at the crack tip for the conventional fibre specimen. The de-bonded length of fibre is no longer constrained from radial deformation by the matrix and so it undergoes radial contraction. This leads to a reduction in the frictional sliding behaviour of the de-bonded length of conventional fibre.

In the case of the auxetic fibre specimen, on the other hand, the negative Poisson's ratio-induced radial expansion of the fibre causes the tip of the de-bond to close up, leading to a reduction in the stress concentration in this region. The tendency of the de-bonded length of auxetic fibre to expand radially ensures contact between the un-bonded fibre and matrix is maximised, leading to an increase in the frictional contact. This is evidenced by the notably rougher B-C region of the load-displacement curve for the auxetic fibre specimen, indicative of slip-stick frictional sliding of the de-bonded region of fibre, and has also been noted in the work on auxetic and conventional copper foam fasteners [32]. Hence, the decreased stress concentration at the de-bond tip, and the increased frictional forces experienced by the de-bonded length of fibre combine to produce a retarded de-bond event for the auxetic fibre specimen. In other words, total de-bonding occurs at a lower displacement during the pull-out test for the conventional fibre specimen (C_c-displacement $\sim$4 mm) than for the auxetic fibre specimen (C_A-displacement $\sim$14 mm)-Figs 7, 8f and g.

The tendency of the matrix to restrict the radial expansion of the de-bonded section of auxetic fibre constrains the axial deformation of the auxetic fibre to occur predominantly along the free fibre section only (Fig. 8d–f). This contrasts with the conventional fibre case where axial deformation will occur predominantly along both the de-bonded and free fibre sections (Fig. 8c–e). Hence, it might be expected that the auxetic fibre would undergo some degree of plastic deformation during the test before the conventional fibre, as a result of accommodating more local strain in the deformable section of fibre (Fig. 8f). This is consistent with the fact that some of the auxetic fibre specimens show clear evidence of yielding (Fig. 5), whereas the conventional fibre specimens do not (Fig. 6).

It is interesting to note that the curve for the conventional fibre shows a small dip followed by an increase at C_c, Fig. 7. The dip possibly represents the reduction in applied force necessary to maintain the displacement rate immediately after the final destruction of the interface. At this point the fibre is essentially free from the matrix and will undergo both shortening along its length and expansion radially as the fibre tends to relax back to its original dimensions (Fig. 8f). The contact and, therefore, frictional forces between the de-bonded fibre and surrounding matrix will thus be increased due to the radial expansion of the fully de-bonded fibre. Hence, the increase in the curve, immediately after the dip, is suggested to correspond to the increase in force

required to overcome the increased friction force associated with the radial expansion of the de-bonded conventional fibre.

In the case of the auxetic fibre specimen, the dip in the curve at C_A is again interpreted as the decrease in force required to maintain constant displacement rate at the point of full failure of the fibre-matrix interface. In this case, however, there is no increase in the curve following the dip. Again, this is explained in terms of the tendency of the fibre to undergo relaxation towards the initial fibre dimensions once full de-bonding has occurred. For the auxetic fibre, the longitudinal contraction of the fibre at the point of full de-bonding is accompanied by a radial contraction due to the negative Poisson's ratio (Fig. 8g). This results in a reduction in contact between the fully de-bonded fibre and matrix, and therefore a reduction in the frictional sliding force. Hence the drop at C_A is likely to be due to two effects, the full failure of the interface and the reduction in friction forces due to radial contraction of the fully de-bonded fibre.

To summarise in terms of frictional contact: the de-bonded section of conventional fibre is in minimal contact during the de-bond event due to the positive Poisson's ratio effect, and increases contact following full de-bonding due to the tendency to return to the original fibre dimensions. For the auxetic fibre, the contact during the de-bond event is increased due to the negative Poisson's ratio, and reduces following full de-bonding as the fibre tends to return to its original dimensions. The contact per unit area once the fibres have relaxed following full de-bond will be approximately equal in both cases since they will both have tried to return to the original fibre dimensions. However, full recovery of the original dimensions will be hindered by the frictional forces acting, and also any plastic deformation that may also have occurred. Fig. 5 provides clear evidence of the tendency for the auxetic fibres to undergo some degree of plastic deformation in the pull-out tests. Since the frictional forces during the de-bond event will be higher for the auxetic fibre then it is unlikely to undergo the same degree of recovery as the conventional fibre following full de-bond. Hence it is expected that a greater length of de-bonded auxetic fibre within the matrix following full de-bond (Fig. 8g), and a correspondingly larger frictional force at any given displacement following full de-bonding are found. This explains the higher force for the auxetic fibre sample for displacements above C_A in Fig. 7. Note however, that the slope of the two curves is similar in this high displacement region (>14 mm), as expected for frictional pull-out.

The area under the load-displacement curve represents the energy required to cause fibre pull-out, and this is over three times greater for the auxetic fibre specimen than for the conventional fibre specimen. Further analysis of the pullout curves reveals that if energy values are calculated separately for the four individual phases, auxetic fibres require 2.3 times more energy for the first 0-A phase, 9.2 times more energy to complete the A-B de-bonding phase, 6.5 times more energy to complete the B-C de-bonding phase and 0.4 times the energy required for the C-D phase (because this phase is so much shorter for the auxetic fibre pullout).

Previously, the anchoring or self-locking properties of auxetic foam materials have been investigated in the design and testing of an auxetic copper foam fastener [32], and also in model calculations using the finite element method [33]. The finite element method has also been employed to study the effects of a negative Poisson's ratio on an elastic plate undergoing tangential tension whilst under constant normal compression between two rigid blocks [34]. In all cases the presence of a negative Poisson's ratio was shown to lead to enhanced anchoring behaviour.

The work reported in this paper extends the previous studies to consider anchoring enhancements in systems employing auxetic fibres. Auxetic fibres have been shown, through experimental comparative testing, to enjoy enhanced fibre pull-out resistance over their conventional counterparts. The results reported here have implications for the use of auxetic fibres in, for example, fibre-reinforced composites [5] and in biomedical applications such as suture or muscle ligament anchors [35].

5. Conclusion

Comparative single fibre pullout tests have been performed on samples containing auxetic and conventional PP fibres. The auxetic and conventional fibres have closely matched diameters and Young's moduli. The auxetic specimens were found to demonstrate higher load over the entire displacement range employed during the test. The auxetic specimens sustained an average maximum load of 0.96 N compared with average maximum load of 0.44 N for the conventional specimens. The total energy required to pull out the auxetic fibre (8.3 mJ) was found to be over 3 times that for the conventional fibre (2.5 mJ). A conceptual model of the fibre pullout process has been presented to explain the essential features of the load-displacement curves and to account for the differences between the two fibre types.

Acknowledgments

The authors would like to acknowledge the support of the EPSRC for funding and Professor E Betz for providing information about experimental and analytical techniques.

References

1. D. R. VERONDA and R. A. WESTMANN, *J. Biomech.* **3** (1970) 111.
2. J. L. WILLIAMS and J. L. LEWIS, *Trans. ASME, J. Biomech. Eng.* **104** (1982) 50.
3. D. J. GUNTON and G. A. SAUNDERS, *J. Mater. Sci.* **7** (1972) 1061.
4. R. LAKES, *Science* **235** (1987) 1038.
5. K. E. EVANS, *Chem. Ind.* (1990) 654.
6. K. L. ALDERSON, A. F. FITZGERALD and K. E. EVANS, *J. Mater. Sci.* **35** (2000) 4039.

7. B. D. CADDOCK and K. E. EVANS, *J Phys. D: Appl. Phys.* **22** (1989) 1877.
8. K. E. EVANS and K. L. AINSWORTH, in International Patent appl. no: WO 91/01210. Publication date 01/02/91.
9. A. P. PICKLES, R. S. WEBBER, K. L. ALDERSON, P. J. NEALE and K. E. EVANS, *J. Mater. Sci.* **30** (1995) 4059.
10. K. L. ALDERSON, A. P. KETTLE, P. J. NEALE, A. P. PICKLES and K. E. EVANS, *ibid.* **30** (1995) 4069.
11. P. J. NEALE, A. P. PICKLES, K. L. ALDERSON and K. E. EVANS, *ibid.* **30** (1995) 4087.
12. A. P. PICKLES, K. L. ALDERSON and K. E. EVANS, *Polym. Eng. Sci.* **36(5)** (1996) 636.
13. K. L. ALDERSON and V. R. SIMKINS, UK Patent appl. No 9905145.0 (1999).
14. K. L. ALDERSON, A. ALDERSON, G. SMART, V. R. SIMKINS and P. J. DAVIES, *Plast, Rubber Compos Process Appl* **31(8)** (2002) 344.
15. K. L. ALDERSON, V. R. SIMKINS and A. ALDERSON, in proceedings of ECCM9 Brighton, (UK, 4–7th June 2000).
16. E. BETZ REPORT, No SETEC-ME 79–34 University of Pittsburgh, (Pittsburgh PA, 1979).
17. J. A. NAIRN, C. H. LIU, D. A. MENDELS and S. ZHANDAROV, in Proceedings of 16th Ann. Tech Conf. Of the Amer. Soc. Composites, VPI, Blacksburg VA, Sept 9–12, 2001.
18. B. P. MILLER, P. MURI and L. REBENFIELD, *Comp. Sci Tech.* **28** (1987) 17.
19. J. A. NAIRN, *Ad Compos Lett* **6** (2000) 373.
20. W. BECKERT and B. LAUKE, *Comp. Sci. Tech.* **57** (1997) 1689.
21. E. PISANOVA, S. ZHANDAROV and E. MÄDER, *Comp. Part A* **32** (2001) 425.
22. C. L. SO and R. J. YOUNG, *Composites Part A* **32** (2001) 445.
23. C. ATKINSON, J. AVILA, E. BETZ and R. E. SMELSER, *J. Mech. Phys. Solids* **3** (1982) 97.
24. C. MAROTZKE, *Comp. Sci Tech.* **50** (1994) 393.
25. V. R. SIMKINS, P. J. DAVIES and K. L. ALDERSON, Paper P3, Int. Conf. Deformation, Yield and Fracture of Polymers, Churchill College, Cambridge, 10-13/4/2000.
26. Ciba data sheet-Araldite LY 5082 resin, Araldite HY 5083 hardener. June 1992.
27. G. DESARMOT and J. P. FAVRE, *Comp. Sci. Tech.* **42** (1991) 151.
28. P. S. CHUA and M. R. PIGGOTT, *ibid.*, **22** (1985) 107.
29. M. R. PIGGOTT and D. ANDISON, *J. Reinf. Plast. Comp.* **6** (1987) 290.
30. L. S. PENN and S. M. LEE, *Fib. Sci. Tech.* **17** (1982) 91.
31. A. TAKAKU and R. G. C. ARRIDGE, *J. Phys. D: Appl. Phys.* **6** (1973) 2038.
32. J. B. CHOI and R. S. LAKES, *Cell. Polymers* **14** (1991).
33. D. W. OVERAKER, A. M. CUITINO and N. A. LANGRANA, *Mech of Mater* **29** (1998) 43.
34. S. V. SHILKO and A. I. STOLYAROV, *J. Friction and Wear* **4** (1996) 23.
35. K. E. EVANS and A. ALDERSON, *Adv. Mater.* **9** (2000) 617.

Received 24 May 2004
and accepted 10 February 2005